

1 **Is the Car Following Behaviour of Human Drivers Affected when**
2 **Following Autonomous Vehicles?**

3 Ruixuan Zhang¹, Sara Masoud², and Neda Masoud³

¹ Graduate Research Assistant, Civil and Environmental Engineering

University of Michigan Ann Arbor

Address: 2350 Hayward St, Ann Arbor, MI 48109

Email: ruixuanz@umich.edu

² Assistant Professor, Industrial and Systems Engineering

Wayne State University

Address: 4815 4th St, Detroit, MI 48201

Email: saramasoud@wayne.edu

³ Assistant Professor, Civil and Environmental Engineering

University of Michigan Ann Arbor

Address: 2350 Hayward St, Ann Arbor, MI 48109

Email: nmasoud@umich.edu

4 **Abstract**

5 The past few years have been witness to an increase in autonomous vehicle (AV) development and
6 testing. However, even with a fully developed and comprehensively tested AV technology, AVs
7 are anticipated to share the roadway network with human drivers for the unforeseeable future. In
8 such a mixed environment, we use naturalistic driving data from the Next Generation Simulation
9 (NGSIM) and Lyft Level 5 (Lyft L5) prediction datasets to investigate whether the existence of AVs
10 influences the car following behavior of human drivers. We use time headway time series as a proxy
11 to capture the car following behaviour of human drivers. We then develop a nested fixed model
12 to find possible changes in behaviour when human drivers are following different types of vehicles

13 (i.e., human-driven vehicles or AVs). The factors included in this model are the platoon structure
14 (a legacy vehicle following a legacy vehicle, and a legacy vehicle following an autonomous vehicle),
15 road type (freeway and urban), time period (morning and afternoon), lane (right, middle, and
16 left), and the source of the data (NGSIM and Lyft L5). Results indicate a statistically significant
17 difference between the car following behaviour of drivers when they follow a human-driven vehicle
18 compared to an AV. This change in the car following behaviour of drivers is manifested in the form
19 of a reduction in the mean and variance of time headways when human drivers follow an AV. These
20 findings can bridge the gap between anticipated and real-world impacts of AVs on traffic streams
21 and roadway stability and capacity, providing meaningful insights on the influence of AVs on the
22 driving behavior of humans in a naturalistic driving environment.

23 **Keywords:** Autonomous vehicle-human driver interactions, Car following behaviour

24 **1 Introduction**

25 The past few years have been witness to an increase in autonomous vehicle (AV) development
26 and testing, with many mobility-oriented companies as well as original equipment manufacturers
27 (OEMs) attempting to either open AV divisions or partner with/acquire start-ups that focus on
28 software or hardware development for AVs. This move toward a future autonomous transportation
29 system is fueled by many anticipated benefits of AVs, such as increased safety and smoother
30 traffic flow, which in turn leads to higher levels of fuel economy, less congestion, and curbing
31 the environmental footprint of the transportation sector [Stern et al. \(2018\)](#). It might, however,
32 take several decades for a fully autonomous transportation system to be deployed. Many experts
33 argue that even with a fully developed and comprehensively tested AV technology, there will still
34 be individuals who either have a distrust in the technology or do not wish to cease driving for other
35 personal reasons. Therefore, it is safe to assume that AVs would have to share the roadway network
36 with human drivers for the unforeseeable future.

37 Since the advent of personal automobiles traffic engineers have been interested in studying the
38 car following behaviour of human drivers, with Bruce Greenshields being credited with the first
39 recorded set of experiments to scientifically measure this car following behaviour [Greenshields et al.](#)
40 [\(1934\)](#). The advent of AVs has given rise to an interesting research question: will the car following

41 behaviour of human drivers be affected when they knowingly follow an autonomous vehicle? Few
42 attempts have been made in the literature to answer this question. [Rahmati et al. \(2019\)](#) set up
43 two sets of experiments with a platoon of size three, where the third vehicle in the platoon was
44 a human-driven vehicle. In the first set of experiments the second vehicle was a human-driven
45 vehicle, and in the second set of experiments it was an AV. They recorded the trajectory of the
46 third vehicle, and used data-driven and model-based approaches to discern any changes in the
47 car following behaviour of the third vehicle in reaction to its preceding vehicle. They concluded
48 that when following an AV, a human driver’s car following behaviour is significantly different than
49 following a human-driven vehicle.

50 Conducting controlled field experiments allows for assessing the impact of a single factor at
51 a time on the car following behaviour of human drivers, while keeping all other factors fixed.
52 However, controlled field experiments have a number of downsides. First, a combinatorial number
53 of experiments are required to capture the impact of multiple factors changing at once. This
54 could easily render comprehensive controlled field experiments impractical, since a wide range of
55 environmental factors as well as the presence of other agents (e.g., other AVs or legacy vehicles,
56 pedestrians, bicycles, etc.) may play a role in the car following behaviour of drivers. As a result,
57 the conclusions obtained from basic and contained field experiments, although insightful, may not
58 be readily generalizable to a naturalistic driving environment. As such, in this paper we seek to
59 investigate the car following behavior of human drivers who follow an AV in a naturalistic driving
60 environment using a naturalistic and large dataset that allows for making statistically significant
61 conclusions. To this end, we use the Lyft Level 5 (Lyft L5) [Houston et al. \(2020\)](#) data repository, in
62 which a fleet of AVs travels on a fixed route in an urban environment, providing over 1,000 hours of
63 AV trajectories, their surrounding agents, and the transportation network. The route encompasses
64 a variety of transportation facility types, including intersections and corridors. This dataset is the
65 first to enable analysis of the car following behaviour of a heterogeneous set of drivers who follow
66 an AV in a naturalistic and dynamically changing driving environment.

67 Despite the benefits of using naturalistic driving data in analyzing the changes in the car
68 following behaviour of human drivers when following an AV, it also poses a unique set of challenges.
69 More specifically, the appearance of an AV is a key factor that can influence a human driver’s car
70 following behavior. For the presence of an AV to change the behaviour of human drivers, they

71 should be able to discern that they are following an AV based on clear visual cues. Garnished by
72 lidars and cameras, AVs generally have a distinctive look that human drivers are likely to discern.
73 Additionally, a human driver’s car following behaviour depends on their subjective opinion on how
74 an AV operates and its risk-taking attitude [Zhao et al. \(2020\)](#). As such, to mitigate the risk of
75 unwanted bias in data collection, data should be collected in an extended period of time from a
76 diverse set of drivers.

77 The car following behaviour of a driver can be reflected using a number of parameters, e.g.,
78 velocity, acceleration, and time headway [Wang et al. \(2014\)](#). Here, we use time headway (THW)–
79 defined as the time it takes for the following vehicle to reach its leading vehicle–to model car
80 following behaviour. As such, we conduct change point analysis on THW of the following driver to
81 identify the moment in time when the human driver has identified its leading AV.

82 The remainder of the paper is organized as follows. In section [2](#) we present the existing work
83 and list the contributions of this paper. In section [3](#) we present our analytical approach in detail.
84 In section [5](#) we lay out our analysis using Lyft L5 and NGSIM datasets and present our findings.
85 We conclude the paper in section [6](#).

86 **2 Literature review**

87 In traffic modeling, the car-following behavior has been intensively studied to establish how a
88 vehicle interacts with its leading vehicle. The main idea is to work with longitudinal dynamics
89 of the vehicle pair, such as velocity, acceleration, time headway, and time-to-collision inverse, to
90 uncover the behavior patterns of the following vehicle in various driving scenarios. There are two
91 main components involved in the study of car-following behavior: modeling and analysis. These
92 two components are discussed in the following.

93 **2.1 Modeling**

94 As the most commonly encountered driving maneuver in the real world, car following behavior has
95 been extensively studied in investigating many specific driving situations. To properly describe the
96 interaction between the leading and following vehicles, several measures are proposed. Time-to-
97 collision (TTC) reflects human drivers’ perception of their safety for potential collision and it is
98 strongly related to longitudinal acceleration/deceleration ([Jin et al., 2011](#)). ([Vogel, 2003](#)) compares

99 time headway and TTC with real-world traffic data and concludes that time headway and TTC are
100 independent but suitable for different usages. They also argue that time headway directly reflects
101 potential danger and thus prevents risky TTC, while TTC should be used for actual danger, i.e.,
102 on-road obstacle or collision. (Boer, 1999) also mentioned that time headway characterizes the
103 safety margin in the situation where the preceding vehicle decelerates while TTC means the time
104 left for drivers to intervene to avoid for a crash. Headway is not considered here as it can not include
105 velocity-related information which is necessary to learn car following behavior. As we are interested
106 in human drivers' reaction to on-road stimuli (the preceding AV) without evaluating an actual
107 collision, time headway works better. Several car-following behavior models are formulated using
108 ordinary differential equations (ODE) that take positions and velocities of vehicles as inputs. The
109 intelligent driving model (IDM) Treiber et al. (2000) and optimal velocity model (OVM) Sugiyama
110 (1999) are two extensively-applied ODE-based models capable of modeling nonlinear dynamics.
111 Additionally, a linearized model can be further derived from ODEs via Taylor expansion. The
112 full velocity difference model (FVDM) Jiang et al. (2001) was developed based on OVM and the
113 generalized force model (GFM) Helbing and Tilch (1998) by taking both positive and negative
114 velocity differences into account. It could obtain more precise predictions of vehicle motion in
115 traffic jam density. Wiedemann 74 (W-74) model and Wiedemann 99 (W-99) model Durrani et al.
116 (2016) are two car-following models developed by Rainer Wiedemann, where the drivers change
117 their behaviors at discrete time steps only when certain thresholds (predefined for headway, speed,
118 or relative speed) are reached. However, the values of parameters in W-99 are empirical, and no
119 literature exists to indicate how ranges for these parameter should be established, which prompted
120 many related works Durrani et al. (2016); Mathew and Radhakrishnan (2010); Gallelli et al. (2017)
121 in calibrating the W-99 model. Newell's car-following model Newell (2002) applied a similar concept
122 to W-99, assuming that a vehicle will maintain a minimum space and time gap between itself and
123 its preceding vehicle. Some studies which pursue a more general way of modeling the car-following
124 behavior are discussed in Ro et al. (2017) and Koutsopoulos and Farah (2012), where not only the
125 car-following dynamics is considered, but also random human factors and different driving scenarios
126 (such as following and emergency braking) were accounted for. Other car-following models such
127 as adaptive cruise control (ACC) and cooperative adaptive cruise control (CACC) were designed
128 for commercial vehicles, applying automated longitudinal control by adjusting acceleration with a

129 linear function to maintain preset velocity and headway values.

130 All of the aforementioned car-following models are based on mathematical formulations with
131 longitudinal dynamics, taking advantage of traditional control theory. On the other hand,
132 predictive techniques enable a data-driven approach and can directly learn the car-following
133 behavior using real-world data. [Zhang et al. \(2008\)](#) utilized time headway and time-to-collision
134 inverse data and a back-propagation neural network to reproduce longitudinal accelerations. A long
135 short-term memory (LSTM) neural network in [Zhang et al. \(2019\)](#) used the position information of
136 surrounding vehicles to predict the car-following behavior with low longitudinal trajectory error. A
137 deep deterministic policy gradient reinforcement learning car-following model was developed in [Zhu
138 et al. \(2018\)](#), where a mapping from speed, relative speed, and headway to acceleration regime of the
139 following vehicle were obtained to deliver a human-like car-following model. A Gaussian mixture
140 model (GMM) was developed in [Angkititrakul et al. \(2011\)](#) to anticipate the future car-following
141 behavior based on velocity and headway. Such learning-based methods require a large amount of
142 training data, and the quality of data significantly influences model performance. Neural network-
143 based designs also require careful tuning when learning the longitudinal dynamics of vehicles [Da Lio
144 et al. \(2020\)](#).

145 From the literature, it can be noticed that multiple longitudinal dynamics impact the car-
146 following behaviors of both the following vehicle and the proceeding vehicle, among which relative
147 distance and velocity are the two most essential factors. To leverage this finding and reduce the
148 complexity of the model, we select time headway as the main feature for modeling car-following
149 behavior as it accounts for both relative distance and velocity ([Chen et al. \(2015\)](#) and [Vogel \(2002\)](#)).

150 **2.2 Analysis**

151 Car-following behavior is of interest to transportation researchers as it can provide insights into the
152 best ways to approach flow throughput control, on-road safety, and energy consumption, etc. There
153 are two directions followed in the current literature to analyze car-following behavior of drivers: one
154 studies the stability (string stability and plant stability) of traffic flow, while the other quantifies
155 the car-following behavior using statistical tools such as mean and variance. As this work focuses
156 on patterns of interactions between human-driven vehicles and AVs, the analysis of string stability
157 and plant stability is out of the scope this study.

158 Car-following behavior may be affected by many factors such as road condition, weather, and
159 vehicle type. When dealing with data relevant to multiple factors, Analysis of Variance (ANOVA)
160 is a powerful tool to investigate the influence level of each factor. In [Liu et al. \(2019\)](#), two one-way
161 ANOVA tests were conducted, indicating that different speed limits have a significant influence on
162 the time headway and headway, and the mean of time headway is closely centered around a fixed
163 value. A factorial ANOVA analysis was conducted in [Hjelkrem \(2015\)](#) to determine the interactions
164 between area type, number of lanes, and vehicle type influencing the car-following behavior. Road
165 condition is suggested to be a critical factor in influencing both headway and time headway by [Wang
166 et al. \(2015\)](#) and [Houchin \(2015\)](#). Significant influence from vehicle type (2-door car v.s. 4-door
167 vehicles, sedans v.s. trucks, vehicles v.s. motorcycles) is also observed in [Evans and Wasielewski
168 \(1983\)](#), [Houchin \(2015\)](#), and [Amini et al. \(2019\)](#).

169 The literature on the analysis of car-following behavior mainly focuses on human-driven vehicles,
170 and AV-involved scenarios are rarely studied. Human-AV interactions at the microscopic level were
171 first studied in [Rahmati et al. \(2019\)](#), where a field experiment was conducted though setting up
172 two two-vehicle platoon structures of human-following-human and human-following-AV. [Rahmati
173 et al. \(2019\)](#) showed that a shorter headway is selected when human drivers follow an AV. Other
174 field experiments conducted by [Zhao et al. \(2020\)](#) suggest that a driver’s subjective attitude toward
175 to AV technology dominates the actual AV’s driving behavior in the speed-headway relationship.
176 Observations from these two field experiments indicate that the limited data collected from field
177 experiments degrades the robustness of the intersection effect(s). Recently, [Li et al. \(2021\)](#) leveraged
178 the Lyft L5 dataset as the data source for operational safety analysis in human-AV interactions
179 in car-following scenarios. In this study we utilize the Lyft L5 and NGSIM datasets to provide
180 a comprehensive and robust evaluation of the car following behaviour of humans, accounting for
181 multiple factors that may affect the car-following behaviour of human drivers. This naturalistic
182 study serves as a necessary complement to the existing field experiments.

183 **2.3 Contributions**

184 The objective of this paper is to provide insights on the potential influence of AVs on the
185 car-following behavior of human drivers. The contributions of this paper are two-fold: (i) we
186 apply statistical analysis on time headway data from Lyft L5, using NGSIM datasets (US101, I-80,

187 Lankershim Blvd) as the control group, to find the influence of leading AVs on the car-following
 188 behaviour of following drivers; (ii) This naturalistic study provides evidence that human drivers
 189 are regulated as a result of introducing AVs, as evidenced by the statistically significant reduction
 190 in the mean value and variance of their time headways.

191 3 Methods

192 The objective of this study is to investigate whether, and the extent to which, the existence of
 193 AVs in the traffic stream influences the car following behaviour of human drivers. To answer this
 194 question, we propose a comprehensive framework demonstrated in Figure 1. Data used in this study
 195 is obtained from two public datasets: Lyft L5 [Houston et al. \(2020\)](#) and NGSIM [NGS \(2021\)](#). We
 196 use time headway time series in our analysis as a proxy to quantify the car-following behaviour of
 197 vehicles. Time headway between two vehicles is defined as the travel time from the centroid of the
 198 following vehicle to the centroid of the preceding/leading vehicle based on the following vehicle’s
 199 speed. In the rest of this paper, we denote a legacy vehicle following an autonomous vehicle as
 200 LFA, and a legacy vehicle following a legacy vehicle as LFL. We refer to LFA and LFL as platoon
 201 structures.

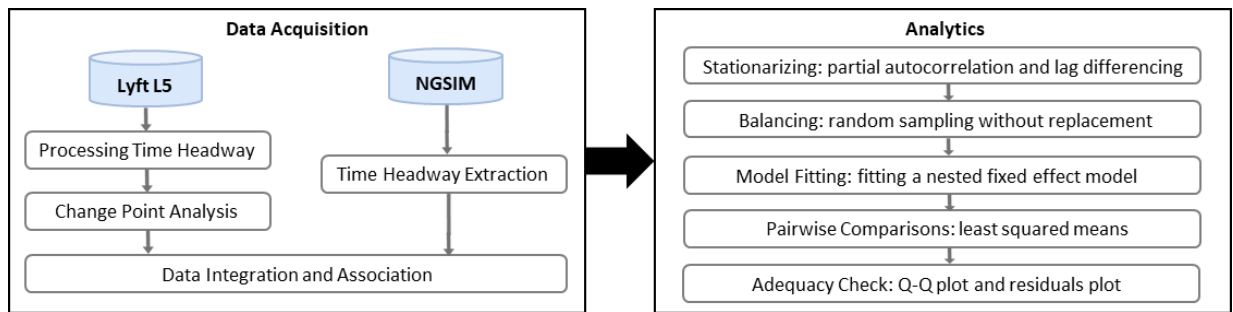


Figure 1: The proposed framework to study the car-following behavior of drivers in LFL and LFA platoon structures.

202 As displayed in Figure 1, the proposed framework consists of two main phases, namely, data
 203 acquisition and data analysis. These phases are described in the following sections.

204 3.1 Phase I: Data Acquisition

205 The first phase starts by extracting time headways of LFL and LFA platoon structures. More
 206 precisely, we extract LFA time headways from the Lyft L5 dataset, and LFL time headways from
 207 both Lyft L5 and NGSIM datasets. Once the time headways are extracted, We use Bayesian change

208 point analysis to filter out the portions of time headway data in the LFA platoon structure where
209 the legacy vehicle is not aware of following an AV.

210 3.1.1 Change Point Analysis

211 Our objective in this study is to make a determination on whether the presence of an AV affects
212 the car following behaviour of its following vehicle in the LFA platoon structure. Consequently, we
213 first need to identify scenarios in the Lyft L5 dataset where a legacy vehicle is following an AV, and
214 more importantly, is *aware* that it is following an AV. To identify such scenarios, we first identify
215 scenes from the Lyft L5 dataset where a legacy vehicle is immediately following an AV. Next, for
216 each scene we use change point analysis to mark any changes in the time headway sequence of the
217 legacy vehicle, and the velocity sequence of its leading AV [Ruggieri and Antonellis \(2016\)](#). The
218 adopted Change point analysis is an online detection approach that provides uncertainty bounds
219 on the number and location of change points across observations [Ruggieri and Antonellis \(2016\)](#).
220 This method strives to make fast inferences on the occurrence of new change points based on each
221 new observation [Ruggieri and Antonellis \(2016\)](#).

222 Let us denote by c_L^h the time instance when a change point is detected in the time headway
223 time series of the legacy vehicle, and by c_A^v the time instance when a change point identified in
224 the velocity time series of the AV. Let us denote by t_{\min}^r and t_{\max}^r the minimum and maximum
225 reaction time of the legacy vehicle, i.e., the time period lapsed from the moment the AV changes
226 its acceleration and the moment the acceleration of the legacy vehicle changes in response. When
227 $t_{\min}^r \leq c_L^h - c_A^v \leq t_{\max}^r$, the change in the time headway of the legacy vehicle can be attributed to
228 its car-following behaviour. However, when c_L^h is not preceded with a c_A^v within the time interval
229 $[t_{\min}^r, t_{\max}^r]$, i.e., the change point analysis detects a change in time headway of the legacy vehicle
230 that cannot be attributed to its car-following behaviour, we postulate that this change can be
231 attributed to the legacy vehicle having identified its proceeding vehicle as an AV, and only consider
232 the trajectory of the legacy vehicle after this change point. In other instances where no such change
233 point is detected, we assume that the legacy vehicle is aware of its leading AV due to the distinctive
234 appearance of AVs in the Lyft L5 study.

235 In the final step of phase I, the collected and filtered time headways from both Lyft L5 and
236 NGSIM datasets are integrated and associated. In this step, each time headway is labeled based

237 on platoon structure, road type, time period, data source, and lane as shown in Figure 2.

238 **3.2 Phase II: Analysis**

239 Phase II focuses on analysis. In the first step, two samples of equal sizes are taken from LFA and
240 LFL datasets. Next, partial autocorrelation analysis is employed to detect autocorrelation lags.
241 Using these identified lags, differencing is applied to stationarize the randomly selected time series.

242 Next, we define the factors of interest, which alongside time headway will be used for fitting the
243 ANOVA model. For human drivers, there is an empirical preferable time headway interval towards
244 the preceding vehicle (Fuller (1981); Das and Maurya (2017)). When time headway is shorter than
245 the lower bound, drivers are more likely to slow down, while when the time headway is longer
246 than the upper bound, drivers may either keep the current speed or accelerate to catch up with
247 the preceding vehicle. The basic idea is that when the time headway is inside the interval, human
248 drivers will feel comfortable and will not overreact unless there is an external disturbance. This
249 preferable time headway is also influenced by many factors (e.g., road configuration, lane, etc.).
250 Generally, there is no universal standard, and this interval can be determined from the observed
251 data itself. We use the distribution of time headway in the LFA dataset to define the preferable
252 time headway.

253 Once the factors of interest are identified and before fitting the nested model, we first create
254 balanced datasets. To obtain balanced datasets we sample time headways without replacement
255 from LFL and LFA datasets so that the same number of data points will be available in each
256 branch of the nested design. Next, the ANOVA model is fitted using balanced datasets. Finally, we
257 confirm the adequacy of the fitted model, and conduct follow-up pair-wise comparisons to isolate
258 the effects that are significantly different, as displayed in Figure 1. The major steps of the analysis
259 are detailed in the following.

260 **3.3 Analysis of Variance**

261 Analysis of Variance (ANOVA) is one of the most well-known statistical tools for evaluating the
262 existence of significant differences between factor levels on a continuous measurement (Tabachnick
263 and Fidell, 2013). A factorial ANOVA can be implemented to examine the impacts of independent
264 categorical factors on a continuous target variable. Factorial ANOVA is an appropriate approach
265 to study whether there exists a statistically significant difference in the time headway patterns

266 of LFA and LFL platoon structures based on different factors and their levels. One of the main
267 requirements of ANOVA is the independence of observations. The underlying sequential and time
268 dependant nature of time series data is a direct violation of this requirement. To address this
269 issue, we apply a two-step data processing procedure. First, we randomly (without replacement)
270 down-sample the time series to remove any potential dependencies. Next, we render the randomly
271 selected time series approximately stationary through differencing to remove auto-correlation.

272 **3.3.1 Stationarity and Partial Auto-Correlation**

273 In time series, auto-correlation is the correlation between two observations at different time
274 stamps, where these observations correlate with themselves repetitively at certain lags. Auto-
275 correlation and partial auto-correlation plots can be used to study the auto-correlation of time series.
276 Although auto-correlation plots can measure and visualize the correlation between observations for
277 a predefined set of lags, they fail to account for the propagation of correlation among successive lags.
278 Partial auto-correlation analysis addresses this problem by isolating the auto-correlation lag. In this
279 work, we use partial auto-correlation plots to identify auto-correlation lags, and apply differencing
280 at the identified lags to stationarize the time headway time series. We discard data points that
281 cannot be stationarized by first level differencing.

282 **3.3.2 Nested Fixed Effect Model**

283 The design of the fitted factorial ANOVA is highly dependent on the structure of the collected data.
284 Fig. 2 displays the factors of interest. A total of five factors are considered in this study. The first
285 factor, platoon structure, models whether the reported time headway profiles belong to an LFL or
286 an LFA pair. The second factor, road type, represents whether the data is collected from an urban
287 road network (i.e., Palo Alto, CA and Lankershim Blvd, CA) or a freeway (i.e., US 101, CA and
288 I-80, CA). The third factor, time period, models whether the data is collected during the morning
289 (i.e., 7:50am - 9:00am) or afternoon (i.e., 4:00pm - 5:30pm) peak period.

290 The fourth factor studies whether the source of the collected data has any significant impact on
291 human driving behavior. Data source is defined as a factor to account for the impact of different
292 data collection techniques and locations in NGSIM and Lyft L5 datasets. The final factor, lane,
293 represents the lane at which the data has been collected. This factor is considered because the
294 lane in which a vehicle travels could impact its car following behaviour. As the number of lanes is

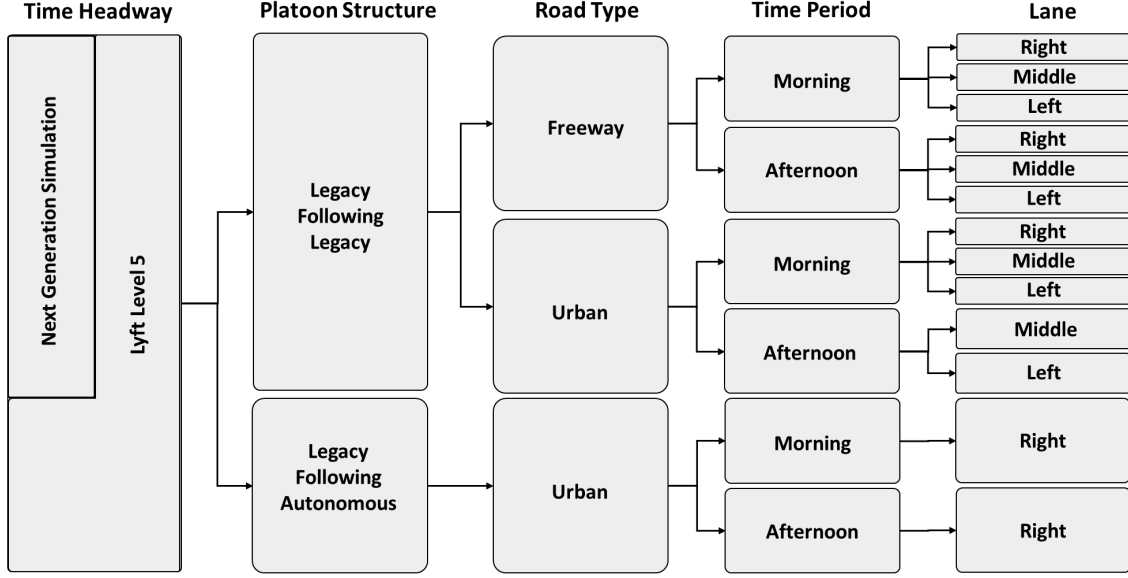


Figure 2: The Structure of the proposed nested model.

295 different across data collection sites, we used one-way ANOVA to group lanes that failed to show a
 296 statistically significant difference in their car following behaviour based on time headway analysis.
 297 As a result, the lane levels simplified to the left (i.e., speeding) lane, the middle lanes, and the right
 298 (merging) lane. Note that the high occupancy vehicle lanes were filtered out in this study when
 299 present.

The factorial ANOVA relies on the underlying relationships between these different factors. Note that AVs are only present in the Lyft L5 dataset and the Lyft L5 data is limited to an urban environment. Furthermore, AV trajectories only appear on the right lane. As such, the values of factors data source, lane, and road type are restricted to the values of the factor platoon structure, leading to the choice of a nested factorial ANOVA as shown in Equation (1).

$$\begin{aligned}
 Y_{l(ijknm)} = & \mu + \alpha_i + \beta_j + (\alpha \times \beta)_{ij} + \gamma_{k(j)} \\
 & + \lambda_{m(j)} + \theta_{n(j)} + \epsilon_{l(ijknm)},
 \end{aligned}$$

for $i, j, k, m \in \{1, 2\}$ and $n \in \{1, 2, 3\}$ (1)

300 where μ represents the overall mean, and $\alpha_i, \beta_j, \gamma_{k(j)}, \lambda_{m(j)}$, and $\theta_{n(j)}$ capture the effects of time
 301 period, platoon structure, data source, road type, and lane, respectively. The parenthetical
 302 subscriptions illustrate the nesting structure of the model. The $(\alpha \times \beta)_{ij}$ models the interaction
 303 effects between factors time period and platoon structure. Here, $\epsilon_{l(ijknm)}$ represents the error

304 term, which is assumed to follow $N(0, \sigma^2)$. In addition to the normality and constant assumptions
 305 regarding the error term, the fitted model should also satisfy the following constraints:

$$\sum_i \alpha_i = 0 \tag{2a}$$

$$\sum_j \beta_j = 0 \tag{2b}$$

$$\sum_i (\alpha \times \beta)_{ij} = 0, \quad \forall j \in \{1, 2\} \tag{2c}$$

$$\sum_j (\alpha \times \beta)_{ij} = 0, \quad \forall i \in \{1, 2\} \tag{2d}$$

$$\sum_k \gamma_{k(j)} = 0, \quad \forall j \in \{1, 2\} \tag{2e}$$

$$\sum_m \lambda_{m(j)} = 0, \quad \forall j \in \{1, 2\} \tag{2f}$$

$$\sum_n \theta_{n(j)} = 0, \quad \forall j \in \{1, 2\} \tag{2g}$$

306 As the nested factorial model in Equation (1) is not identifiable, the additional sets of constraints
 307 in Equation (2) help narrow down the solution space to a unique set of fitted parameters. Using a
 308 single ANOVA model, we define several hypotheses tests to assess the significance of each factor,
 309 with the null hypothesis in each case indicating that the mean time headways are similar for different
 310 values of a given factor, and the alternative hypothesis indicating otherwise. Nested factors (i.e.,
 311 data source, lane, and road type) are added to absorb some of the unexplained variability. As a
 312 result, specific hypothesis tests associated with nested factors are of lesser importance.

313 Although a rejection of the null hypothesis in the ANOVA analysis signals the existence of
 314 a significant effect (i.e., factor), it fails to identify the factor level that is significantly different,
 315 specifically in the presence of interaction effects. As a result, ANOVA analyses are usually followed
 316 by pairwise comparisons. While studying the effects of multiple factor levels, comparisons between
 317 the individual means of either factor may be made using any pairwise comparison technique. We
 318 use Least Square Means to investigate the significance of the factors and apply Tukey's HSD method
 319 to adjust the significance level [Abdi and Williams \(2010\)](#).

320 Multiple assumptions are made prior to fitting the nested fixed effect model. As a result, the
 321 adequacy of the model relies on whether these assumptions hold true. These assumptions include

322 1) the normality of the residuals, i.e., $\epsilon_{l(ijknm)} \sim N(0, \sigma^2)$, and 2) the homogeneity of the residuals.
323 Many mathematical tests are developed for checking the normality and homogeneity of the residuals
324 (e.g., the Shapiro-Wilk test). One problem with such tests is that as the sample size increases, the
325 test results are more likely to fail for even minor departures from normality or homoscedasticity.
326 Therefore, in this paper we rely on visualization approaches instead.

327 4 Data

328 The raw data within both repositories are collected using different sensors such as digital video
329 cameras, radars and lidars.

330 4.1 Lyft L5 Dataset

331 The Lyft L5 Prediction data repository was released by the Lyft Level 5 team in June 2020 [Houston](#)
332 [et al. \(2020\)](#). This data repository contains raw camera/lidar/radar data collected from a fleet of
333 23 AVs operating along a fixed high-demand route in Palo Alto, CA, from October 2019 to March
334 2020. An internal perception stack has already been applied to report information such as the
335 vehicle position based on a global coordinate system, velocity, and a unique ID for each agent. We
336 extract the time headway series of each legacy vehicle in an LFA platoon structure for the purpose
337 of this study.

338 4.2 NGSIM Dataset

339 The Next Generation Simulation (NGSIM) is a well known dataset published by the U.S.
340 Department of Transportation Intelligent Transportation Systems Joint Program Office (JPO) [NGS](#)
341 [\(2021\)](#). This dataset includes detailed vehicle trajectory data collected in four sites: southbound
342 US 101 and Lankershim Boulevard in Los Angeles, CA, eastbound I-80 in Emeryville, CA, and
343 Peachtree Street in Atlanta, Georgia. The data is collected in different time periods from April
344 20, 2005 to November 9, 2006. The dataset contains vehicle ID, global coordinates of the vehicle,
345 vehicle type, velocity, acceleration, space headway, and time headway, among other attributes. We
346 extract the time headway series of each vehicle in each regular (non-carpool) lane at each site for
347 the purpose of this study.

4.3 Data Processing Pipeline

To fully leverage the abundant data in the Lyft L5 and NGSIM datasets for ANOVA, a modular data processing pipeline is developed with three blocks: time headway calculation, change point analysis, and down-sampling and filtering. A detailed explanation of the processing pipeline is given for the Lyft L5 dataset.

- Time headway calculation: Realizing that the driving behavior in different lanes on the same road may be different, the lane-specific time headway data is of our interest. To stay consistent with the NGSIM dataset, all the raw data in the L5 dataset is taken from the multi-lane roads. By utilizing the provided semantic map with 8,500 discrete lane segments, a customized semantic map is constructed by connecting any lanes that physically belong to the same continuous lane (multiple lane segments in the original semantic map may correspond to the same lane in the real world), referred as the augmented map. In the multi-lane roads, three lanes are identified (right lane, middle lane, and left lane). Given the position information of vehicles, the augmented map can immediately match the vehicles to the corresponding lanes. The time headway in the car-following mode is calculated as the travel time from the centroid of the following vehicle to the centroid of the preceding/leading vehicle based on the following vehicle's speed.
- Change point analysis: In investigating an AV's effect on the following behaviour of human drivers, we need to construct a dataset in which the following human driver is aware that the leading vehicle is an AV. To this end, we conduct a change point analysis as described in section 3.1.1.
- Down-sampling and filtering: The sampling frequency in both datasets is 10 Hz, and a high correlation among data points is present under such a high-frequency sampling regime. To ensure independence of observations, autocorrelation and partial autocorrelation are evaluated, and down-sampling of the time headway sequence is implemented. According to our evaluation results, 1 Hz is selected to be the updated sampling frequency. Furthermore, a filtering step is introduced to ensure that the time headway sequence satisfies the minimum length of containing at least 10 data points or 10-seconds of observation.

376 For the NGSIM dataset, as the lane information is readily available, only the down-sampling
377 and filtering module will be used.

378 **5 Results and Discussion**

379 In this section, we present the results of our proposed framework. In accordance with the flow of
380 the framework, we first stationarize the time headway time series through differencing and partial
381 auto-correlation analysis. Then, we balanced our dataset. Next, we test our hypotheses using
382 nested factorial ANOVA, followed by pairwise comparisons.

383 **5.1 Down-sampling and Auto-correlation Analysis**

384 Since the sample frequency in Lyft L5 and NGSIM datasets is high (10 Hz), data points may
385 correlate with each other at such high frequency and thus introduce unnecessary bias into the
386 results. A common approach to reduce autocorrelation is to down-sample the data at a slower
387 frequency. We test Autocorrelation Function (ACF) and Partial Autocorrelation Function (PACF)
388 at down-sampling frequencies of 2Hz and 1Hz, in comparison with the original data. Decreasing
389 sample frequency can significantly reduce both ACF and PACF at higher lags. Down-sampling
390 at 1 Hz can reduce the magnitude of the auto-correlation lags. Differencing at lag one further
391 stationarizes the time series. As the majority of the time series are not significantly auto-correlated
392 after lag 1 differencing, the non-stationary ones are dropped at this step.

393 Some interesting takeaways may be discussed before presenting the ANOVA results. In a freeway
394 driving environment, e.g., US 101 and I-80, after down-sampling at 1 Hz, there is still a significant
395 autocorrelation at lag 1 and neutrally-distributed partial autocorrelation (PAC) after lag 2. In
396 an urban driving environment, Lankershim Blvd and Lyft L5, a similar pattern can be observed;
397 however, at lag 1, a relative smaller ratio of data is correlated. An interpretation for this difference is
398 that in freeways, human drivers encounter fewer external disturbances and therefore their behavior
399 is more consistent and predictable. A neutral-distributed outbound PAC after lag 2 indicates that
400 the behaviors tend to be random in 2 seconds into the future. If we view a human driver as a
401 controller, s/he will control the time headway to the leading vehicle roughly at some period, which
402 can be determined by the lag where outbound PAC values are approximately neutral-distributed.

403 5.2 Factorial Analysis

404 The processed dataset contains a total of 537,060 data points, out of which 5,774 (i.e., 1%) of
 405 data points represent the LFA structure while the remaining 531,285 (i.e., 99%) belong to the LFL
 406 platoon structure. In order to maximize the power of the factorial analysis, the dataset should
 407 be balanced. In addition, balancing helps protect the analysis against small departures from the
 408 assumptions. Although the balancing effort reduces the total size of the dataset (i.e., 25 data points
 409 per each leaf in Figure 2) through random sampling, it improves the the distribution of the data
 410 within different factor levels, including platoon structure: 85% for LFL and 15% LFA; Road type:
 411 46% for freeway and 54% urban; Time period: 53% for morning and 45% afternoon; Lane: 31%
 412 for left, 31% for middle and 38% right.

413 The nested factorial ANOVA introduced in Equation 1 is fitted and its results are displayed in
 414 Table 1. The fitted model allows us to study whether there are statistically significant associations
 415 between the time headway and the factors introduced in Figure 1. Table 1 reports findings on
 416 the main effects (i.e., time period and platoon structure factors), nested effects (i.e., data source,
 417 road type, and lane factors), as well the interaction effects between the time period and platoon
 418 structure factors.

Table 1: Results of the nested fixed model

Factor	DoF	SSE	MSE	F Statistics	P-Value	α
Time Period	1	1.46	1.46	1.55	0.21	0.001
Platoon Structure	1	49.86	49.86	52.81	2.88e-12	
Platoon Structure \times Time	1	1.09	1.09	1.16	0.28	
Platoon Structure: Data Source	1	0.03	0.03	0.04	0.85	
Platoon Structure: Road Type	1	1.92	1.92	2.03	0.15	
Platoon Structure: Lane	2	0.01	0.006	0.006	0.99	
Residuals	317	299.28	0.94			

419 The first three rows in Table 1 correspond to hypotheses on time period, platoon structure,
 420 and the interaction effect between time period and platoon structure factors. The next three rows
 421 display the impact of data source, road type, and lane as nested factors of platoon structure,
 422 respectively. The last row provides some information regarding the residuals. For each one of the
 423 hypotheses of interest, Table 1 reports the degree of freedom (DoF) of the test, sum of squared
 424 errors (SSE), mean square errors (MSE), as well as the F-statistics, its corresponding p-value,
 425 and the significance level at which a conclusion is made. The reported p-values can assess the

426 null hypotheses and determine whether the association between the time headway and the factors
427 of interest are statistically significant. Table 1 reports that only the platooning structure is of
428 significance at $\alpha = 0.001$. The results also highlights the fact that the collected time headway data
429 are not impacted by the differences in data collection techniques and locations in NGSIM and Lyft
430 L5 datasets at a statistically significant level. To further study the results reported in Table 1,
431 multiple follow up pairwise comparisons are conducted to understand which levels of the platoon
432 structure factor are significantly different given the nested structure. Table 2 illustrates the results
433 of the pairwise comparisons.

Table 2: Pairwise comparisons using least square means

	Estimate	SE	T Ratio	P-Value	α
Time Period (Morning vs Afternoon) : Platoon Structure (LFL vs LFA)					
Morning LFL - Afternoon LFL	-0.132	0.132	-0.996	0.7519	
Morning LFL - Morning LFA	0.944	0.215	4.39	0.0001	0.001
Morning LFL - Afternoon LFA	1.055	0.215	4.91	<.0001	0.001
Afternoon LFL - Morning LFA	1.075	0.218	4.93	<.0001	0.001
Afternoon LFL - Afternoon LFA	1.187	0.218	5.44	<.0001	0.001
Morning LFA - Afternoon LFA	0.112	0.275	0.40	0.9774	
Lane (Left vs Middle vs Right) : Platoon Structure (LFL vs LFA)					
Left LFL - Middle LFL	0.013	0.138	0.098	0.9997	
Left LFL - Right LFL	0.016	0.158	-0.103	0.9996	
Left LFL - Right LFA	1.073	0.0171	6.279	<.0001	0.001
Middle LFL - Right LFL	-0.003	0.160	-0.022	1.000	
Middle LFL - Right LFA	1.061	0.171	6.279	<.0001	0.001
Right LFL - Right LFA	1.057	0.191	6.20	<.0001	0.001

434 Although the platoon structure is the only significant factor as reported in Table 1, the
435 interaction effect between time period and platoon structure and the nesting factors may have
436 obscured the comparisons between the means of different levels of the platoon structure. As a result,
437 the least squared method is applied to the means of one of the factors, with the remaining factor
438 set at a particular level. In addition, as pairwise comparisons lead to inflation of the significance
439 level, the p-values within Table 2 are adjusted based on the Tukey method for comparing a family
440 of multiple estimators.

441 Table 2 reports the estimated difference between means (i.e., estimate), the standard error of
442 that estimate (i.e., SE), the T ratio, and its corresponding p-value along with the reported level
443 of significance α . The top half of Table 2 studies the pairwise comparisons between time period
444 and platoon structure. Here, results are averaged over the levels of lane (i.e., left, middle, and

445 right), road type (i.e., freeway and urban), and data source (i.e., NGSIM and Lyft L5). As shown
 446 in Table 2, other than the Morning LFL - Afternoon LFL and Morning LFA - Afternoon LFA, the
 447 remaining levels between time period and platoon structure are significant.

448 The bottom half of Table 2 studies the interaction between the nested factor lane and the main
 449 factor platoon structure. Here, results are averaged over the levels of time period (i.e., morning and
 450 afternoon), road type (i.e., freeway and urban), and data source (i.e., NGSIM and Lyft L5). This
 451 table demonstrates that while the LFL behavior does not significantly differ within the middle,
 452 left, and right lanes, it does significantly differ within the left and right, middle and right, as well
 453 as right and right lanes when compared to LFA. It also shows that although LFL and LFA display
 454 statistically different behaviors in different lanes, they do exhibit statistically significantly different
 455 behaviors even within the same right lane. Although the proposed nested factorial model recognizes
 456 platooning structure leads to a statistically significant different car-following behaviour, and the
 457 follow-up pair-wise comparisons further confirm this, none of these approaches can identify whether
 458 the THW of LFA is less than or greater of LFL's THW. Figure XX demonstrates that LFL has
 459 higher mean and variance THW values when compared to LFA.

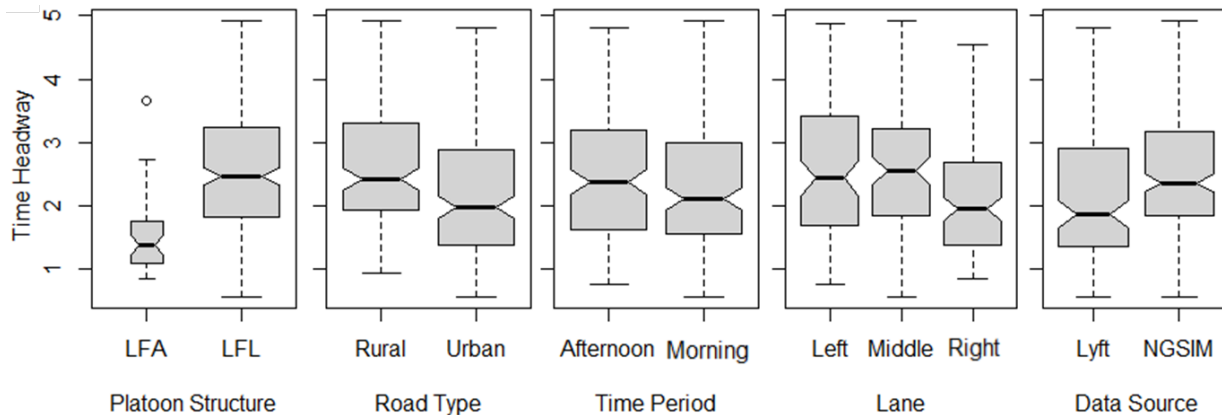


Figure 3: The distribution of time headway over factor levels.

460 As displayed in Figure 2, LFA has lower median (1.38), mean (0.41), and variance (0.31) values
 461 in comparison to LFL which has scores of median (2.48), mean (0.85), and variance (1.05). The
 462 reduction in the mean time headway manifests in less bumper-to-head distance, enabling more
 463 vehicles to operate on the road and increasing the road capacity. The reduction in the variance of
 464 time headway leads to a more stable traffic flow.

465 The final step is the verification of the fitted model’s adequacy through Q-Q and residuals
466 plots as shown in Figure 4. To check the adequacy of the model, Q-Q plots of residuals and
467 residuals versus fitted values are shown in Figure 4. Q-Q plots are commonly used to confirm the
468 normality of the residuals, i.e., $\epsilon_{l(ijknm)} \sim N(0, \sigma^2)$. As a Q-Q plot is a scatter plot created by
469 plotting the actual quantiles of the residuals of the fitted model against the theoretical normally
470 distributed ones, a diagonal line is a confirmation that both sets of quantiles came from the same
471 distribution. In the Q-Q plot in Figure 4, the residuals roughly lie around the 45-degree line,
472 suggesting that they are approximately normally distributed. The homogeneity of the residuals
473 can be validated using the residuals plot. If the variance of the error term is homogeneous, not
474 only should the residuals plot show no pattern, but also the spread of residuals should be equal per
475 group across corresponding fitted values. The residuals plot in Figure 4 show that the variances are
476 approximately homogeneous since the residuals are distributed approximately equally above and
below zero.

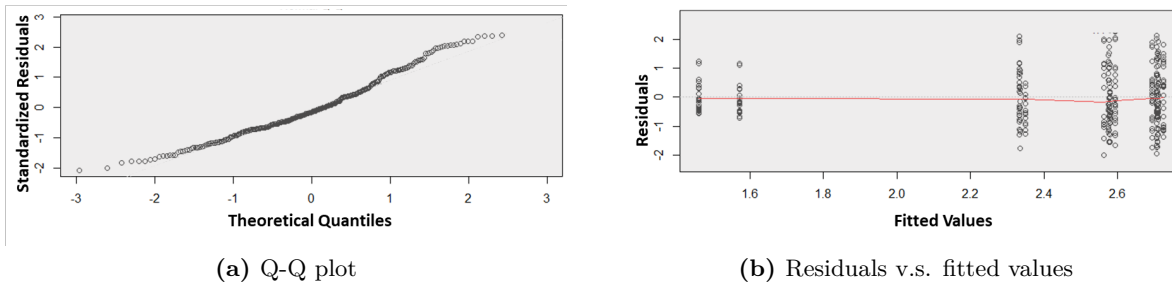


Figure 4: Adequacy check of the fitted nested fixed effect model

477

478 6 Conclusions

479 In this study we proposed a nested factorial model to study the potential effects of autonomous
480 vehicles on human drivers’ car-following behavior using naturalistic driving data (i.e., NGSIM and
481 Lyft L5 prediction datasets). The objective of this study was to bridge the gap between anticipated
482 and real-world impacts of AVs on traffic streams and roadway safety and capacity. The proposed
483 nested model studied the impact of different factors such as platoon structure (i.e., whether a human
484 driver follows a legacy vehicle or an AV), time period, traveling lane, and road type on the time
485 headway between two vehicles, which is considered as a proxy for the car following behaviour of the

486 following vehicle. The results indicate that the platoon structure affects the car following behavior
487 of human drivers in a statistically significant manner, allowing us to conclude that in a real-world
488 setting, a human driver’s car following behaviour when following a legacy vehicle is different from
489 following an autonomous vehicle. Furthermore, our analysis illustrates that the difference in car
490 following behaviour is significantly present regardless of the traveling lane or the time period.

491 **Data Availability Statement**

492 Some of models, or code that support the findings of this study are available from the
493 corresponding author upon reasonable request; All data used during the study are available in
494 repositories online in accordance with funders data retention policies.

495 **Acknowledgments**

496 This work has been supported by Midwest US-DOT Center for Connected and Automated
497 Transportation (award number: 69A3551747105) and National Science Foundation (award number:
498 1837245).

499 **References**

- 500 (2021). U.s. department of transportation federal highway administration. (2016) next generation
501 simulation (ngsim) vehicle trajectories and supporting data. [dataset]. provided by its datahub
502 through data.transportation.gov. <http://doi.org/10.21949/1504477> Accessed May 1.
- 503 Abdi, H. and Williams, L. J. (2010). Tukey’s honestly significant difference (hsd) test. *Encyclopedia*
504 *of research design*, 3(1):1–5.
- 505 Amini, E., Tabibi, M., Khansari, E. R., and Abhari, M. (2019). A vehicle type-based approach
506 to model car following behaviors in simulation programs (case study: Car-motorcycle following
507 behavior). *IATSS research*, 43(1):14–20.
- 508 Angkititrakul, P., Miyajima, C., and Takeda, K. (2011). Modeling and adaptation of stochastic
509 driver-behavior model with application to car following. In *2011 IEEE Intelligent Vehicles*
510 *Symposium (IV)*, pages 814–819. IEEE.
- 511 Boer, E. R. (1999). Car following from the driver’s perspective. *Transportation Research Part F:*
512 *Traffic Psychology and Behaviour*, 2(4):201–206.

513 Chen, X. M., Li, L., and Shi, Q. (2015). A markov model based on headway/spacing distributions.
514 In *Stochastic Evolutions of Dynamic Traffic Flow*, pages 49–79. Springer.

515 Da Lio, M., Bortoluzzi, D., and Rosati Papini, G. P. (2020). Modelling longitudinal vehicle dynamics
516 with neural networks. *Vehicle System Dynamics*, 58(11):1675–1693.

517 Das, S. and Maurya, A. K. (2017). Time headway analysis for four-lane and two-lane roads.
518 *Transportation in developing economies*, 3(1):9.

519 Durrani, U., Lee, C., and Maoh, H. (2016). Calibrating the wiedemann’s vehicle-following model
520 using mixed vehicle-pair interactions. *Transportation research part C: emerging technologies*,
521 67:227–242.

522 Evans, L. and Wasielewski, P. (1983). Risky driving related to driver and vehicle characteristics.
523 *Accident Analysis & Prevention*, 15(2):121–136.

524 Fuller, R. G. (1981). Determinants of time headway adopted by truck drivers. *Ergonomics*,
525 24(6):463–474.

526 Gallelli, V., Iuele, T., Vaiana, R., and Vitale, A. (2017). Investigating the transferability of
527 calibrated microsimulation parameters for operational performance analysis in roundabouts.
528 *Journal of Advanced Transportation*, 2017.

529 Greenshields, B. D., Thompson, J., Dickinson, H., and Swinton, R. (1934). The photographic
530 method of studying traffic behavior. In *Highway Research Board Proceedings*, volume 13.

531 Helbing, D. and Tilch, B. (1998). Generalized force model of traffic dynamics. *Physical review E*,
532 58(1):133.

533 Hjelkrem, O. A. (2015). Determining influential factors on the threshold of car-following behavior.
534 Technical report.

535 Houchin, A. J. (2015). An investigation of freeway standstill distance, headway, and time gap data
536 in heterogeneous traffic in iowa.

537 Houston, J., Zuidhof, G., Bergamini, L., Ye, Y., Chen, L., Jain, A., Omari, S., Iglovikov, V., and
538 Ondruska, P. (2020). One thousand and one hours: Self-driving motion prediction dataset. *arXiv*
539 *preprint arXiv:2006.14480*.

540 Jiang, R., Wu, Q., and Zhu, Z. (2001). Full velocity difference model for a car-following theory.
541 *Physical Review E*, 64(1):017101.

542 Jin, S., Huang, Z.-y., Tao, P.-f., and Wang, D.-h. (2011). Car-following theory of steady-state traffic

543 flow using time-to-collision. *Journal of Zhejiang University-SCIENCE A*, 12(8):645–654.

544 Koutsopoulos, H. N. and Farah, H. (2012). Latent class model for car following behavior.
545 *Transportation research part B: methodological*, 46(5):563–578.

546 Li, T., Han, X., Ma, J., Ramos, M., and Lee, C. (2021). Operational safety of automated
547 and human driving in mixed traffic environments: A perspective of car-following behavior.
548 *Proceedings of the Institution of Mechanical Engineers, Part O: Journal of Risk and Reliability*,
549 page 1748006X211050696.

550 Liu, T. et al. (2019). Comparison of car-following behavior in terms of safety indicators between
551 china and sweden. *IEEE Transactions on Intelligent Transportation Systems*, 21(9):3696–3705.

552 Mathew, T. V. and Radhakrishnan, P. (2010). Calibration of microsimulation models for
553 nonlane-based heterogeneous traffic at signalized intersections. *Journal of Urban Planning and*
554 *Development*, 136(1):59–66.

555 Newell, G. F. (2002). A simplified car-following theory: a lower order model. *Transportation*
556 *Research Part B: Methodological*, 36(3):195–205.

557 Rahmati, Y., Khajeh Hosseini, M., Talebpour, A., Swain, B., and Nelson, C. (2019). Influence of
558 autonomous vehicles on car-following behavior of human drivers. *Transportation research record*,
559 2673(12):367–379.

560 Ro, J. W., Roop, P. S., Malik, A., and Ranjitkar, P. (2017). A formal approach for modeling
561 and simulation of human car-following behavior. *IEEE transactions on intelligent transportation*
562 *systems*, 19(2):639–648.

563 Ruggieri, E. and Antonellis, M. (2016). An exact approach to bayesian sequential change point
564 detection. *Computational Statistics & Data Analysis*, 97:71–86.

565 Stern, R. E., Cui, S., Delle Monache, M. L., Bhadani, R., Bunting, M., Churchill, M., Hamilton,
566 N., Pohlmann, H., Wu, F., Piccoli, B., et al. (2018). Dissipation of stop-and-go waves via
567 control of autonomous vehicles: Field experiments. *Transportation Research Part C: Emerging*
568 *Technologies*, 89:205–221.

569 Sugiyama, Y. (1999). Optimal velocity model for traffic flow. *Computer Physics Communications*,
570 121:399–401.

571 Tabachnick, B. G. and Fidell, L. S. (2013). Using multivariate statistics upper saddle river.

572 Treiber, M., Hennecke, A., and Helbing, D. (2000). Congested traffic states in empirical observations

573 and microscopic simulations. *Physical review E*, 62(2):1805.

574 Vogel, K. (2002). What characterizes a “free vehicle” in an urban area? *Transportation research*
575 *part F: traffic psychology and behaviour*, 5(1):15–29.

576 Vogel, K. (2003). A comparison of headway and time to collision as safety indicators. *Accident*
577 *analysis & prevention*, 35(3):427–433.

578 Wang, J., Xiong, C., Lu, M., and Li, K. (2015). Longitudinal driving behaviour on different roadway
579 categories: an instrumented-vehicle experiment, data collection and case study in china. *IET*
580 *Intelligent Transport Systems*, 9(5):555–563.

581 Wang, W., Xi, J., and Chen, H. (2014). Modeling and recognizing driver behavior based on driving
582 data: A survey. *Mathematical Problems in Engineering*, 2014.

583 Zhang, L., Wang, J., Li, K., Yamamura, T., Kuge, N., and Nakagawa, T. (2008). Driver car-
584 following behavior modeling using neural network based on real traffic experimental data. In *15th*
585 *World Congress on Intelligent Transport Systems and ITS America’s 2008 Annual MeetingITS*
586 *AmericaERTICOITS JapanTransCore*.

587 Zhang, X., Sun, J., Qi, X., and Sun, J. (2019). Simultaneous modeling of car-following and lane-
588 changing behaviors using deep learning. *Transportation research part C: emerging technologies*,
589 104:287–304.

590 Zhao, X., Wang, Z., Xu, Z., Wang, Y., Li, X., and Qu, X. (2020). Field experiments on longitudinal
591 characteristics of human driver behavior following an autonomous vehicle. *Transportation*
592 *research part C: emerging technologies*, 114:205–224.

593 Zhu, M., Wang, X., and Wang, Y. (2018). Human-like autonomous car-following model with deep
594 reinforcement learning. *Transportation research part C: emerging technologies*, 97:348–368.